New Physics: Sae Mulli,
Vol. 69, No. 2, February 2019, pp. 142∼148
http://dx.doi.org/10.3938/NPSM.69.142

Nuclear Magnetic Relaxation of the ^{51}V Nucleus in a YVO_4:Nd Single Crystal

Tae Ho Yeom*
Department of Laser and Optical Information Engineering, Cheongju University, Cheongju 28503, Korea

Sung Soo Park
Department of Science Education and Nuclear Magnetic Resonance Research Center, Jeonju University, Jeonju 55069, Korea

(Received 10 December 2018 : revised 31 December 2018 : accepted 2 January 2019)

Nuclear magnetic resonance data of the ^{51}V nucleus in an YVO_4 single crystal doped with Nd are obtained using a Fourier-transform nuclear magnetic resonance (NMR) spectrometer in the temperature range of 180 K ∼ 410 K. The spin–lattice relaxation mechanisms are investigated, and the dominant mechanism at temperatures above 280 K is found to be the Raman process because the spin lattice relaxation rate of the ^{51}V nucleus is proportional to the square of the temperature ($T_1^{-1} \propto T^2$). However, at temperature below 280 K, the effect of the paramagnetic impurity becomes more significant than that of the quadrupole relaxation. This is verified through an analysis of the activation energy of the paramagnetic Nd^{3+} impurity.

PACS numbers: 76.60.-k
Keywords: Nuclear magnetic resonance, YVO_4:Nd single crystal, Relaxation mechanism, Nd paramagnetic impurity

I. INTRODUCTION

Compact laser diode (LD) working in the visible as well as infrared regions has extensive applications in the industrial fields, therapeutic, military, and scientific research because of their advantages regarding enhanced efficiency, compactness, stability, lifetime and beam quality [1,2]. Such lasers are often created by rare-earth doping of appropriate host crystals.

For instance, beam displacers, polarizers and optical isolators are applications of pure YVO_4 single crystal owing to its large birefringence [3, 4]. YVO_4:Nd single crystal is an excellent laser material currently used in laser diode (LD) pumped solid-state laser for electronics and optical applications. Compared to Nd:YAG (Yttrium Aluminum Garnet: $Y_3Al_5O_{12}$), it has superior laser characteristics such as low lasing threshold, high slope efficiency, and low temperature dependence of pump wavelength [5–10]. The Nd-doped YVO_4 single crystal (1 at% of Nd) exhibit a high optical transparency and a high absorption coefficient at 400 - 5000 nm, and a large stimulated emission cross section of about 3×10^{-13} cm^2 which is several times larger than that of Nd:YAG. Since the fluorescence life time is as short as 90 μs, it is a suitable material for continuous wave (CW) oscillation [7]. Owing to the strong birefringence characteristic of YVO_4:Nd crystal, linearly polarized emission can be obtained.

Since the report of LD excited high lasing efficiency (slope efficiency: about 50 ∼ 60%), YVO_4:Nd has been attracting attention [7]. However, it is very challenging to obtain a high quality YVO_4:Nd single crystal because of the difficulty in crystal growing. The YVO_4:Nd single crystal has been grown using various methods including the Verneuil method, the Flux method, and the Czochralski method from the end of the 1960's [11–13]. Since V_2O_5 evaporates easily during growth, the crystal composition was not congruent, making it challenging to obtain high quality YVO_4:Nd single crystals. The YVO_4:Nd laser has thermal problems and does not exceed the practicality of Nd:YAG lasers. This disadvantage has been alleviated by the LD excitation method,

*E-mail: thyeom@cju.ac.kr

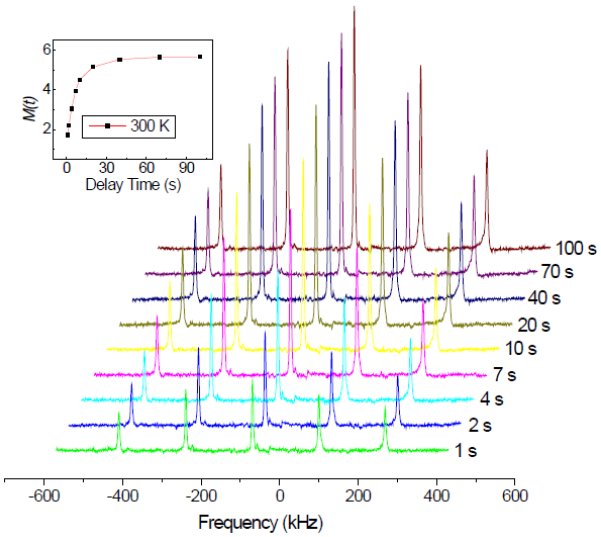

Fig. 1. (Color online) The saturation recovery traces for the ^{51}V nucleus in a YVO_4:Nd single crystal as a function of delay time at 300 K.

and therefore the necessity of high quality YVO_4:Nd single crystal growth has arisen [14].

Lasing properties are highly influenced by the concentration of the impurity ion in solid-state laser materials. The degradation of lasing properties is more likely to occur due to self-quenching when the dopant concentration is exceedingly high. Nevertheless, the increase in the concentration of active ion in the host single crystal can improve lasing properties by allowing a lower threshold and a higher efficiency emission. This stems from the enhancement in efficiency of excitation light absorption [15]. The color of the YVO_4:Nd crystal can vary according to different authors. One of the reasons responsible for this variation is the vacancy of oxygen. Another factor is the different optical sources used. Often, the slightest variation in growth conditions or raw materials processing gives different crystal colors [16].

Yttrium vanadate (YVO_4) single crystal occupies a tetragonal crystal with a point group of 4/mmm and a space group of $I4_1/amd$ (D_{4h}^{19}). The parameters of the cell are $a = b = 7.118$ and $c = 6.293$) [14]. The structure consists of alternating VO_4 tetrahedra and VO_8 bisdisphenoids chains [17]. The single crystal structure of YVO_4 is shown in Fig. 1 of the previous reports [18, 19]. A YO_8 bisdisphenoid has two different sets of Y–O bond lengths and the VO_4 tetrahedron is slightly elongated. YVO_4, $5Y_2O_3$-V_2O_5, and $4Y_2O_3$-V_2O_5 are typical phases of Y_2O_5-V_2O_5 system during the growth of YVO_4 single crystal. YVO_4 has a melting point of 1810 ± 10 °C and therefore the YVO_4 single crystal is generally grown at a temperature above 1810 °C.

The spin lattice relaxation time (T_1) of the ^{51}V nucleus in YVO_4:Nd measures the dynamic nature such as the nuclear phonon interaction as well as paramagnetic impurity effects. It shows how the nuclear system of ^{51}V can easily dispose of its excited state energy to the crystal lattice. In this study, the nuclear magnetic resonance (NMR) spectra of ^{51}V in YVO_4:Nd single crystal were measured using a Fourier transform (FT) NMR spectrometer at 180 K ∼ 410 K. The resonance frequency, linewidth, and the spin-lattice relaxation time of ^{51}V nucleus were obtained as a function of temperature. The spin-lattice relaxation mechanism of the ^{51}V nucleus was explored in the aforementioned temperature range. Also, the phonon interaction as well as the influence of paramagnetic dopant ion on the relaxation of ^{51}V are discussed. The activation energy (E_a) of the ^{51}V nucleus was obtained at two different temperature ranges.

II. EXPERIMENTS

YVO_4:Nd single crystal was grown by the Czocrhalski method in our laboratory. It used 50.7% Y_2O_5 (99.999%), 49.3% V_2O_5 (99.995%) and 1 at% Nd_2O_3 (99.999%) as starting materials. They were mixed and calcined at 1100 °C for 2 hours, then used for single crystal growth. An Ir crucible was used for single crystal growth, and the growth temperature was about 1815 °C. During the growth of YVO_4:Nd single crystal, nitrogen gas of 1.5 atmospheric pressure containing 1% oxygen was used to suppress the volatilization of V_2O_5. The crystal pulling rate and rotation speed were 2 mm/h and 5 rpm, respectively. Annealing after growth of YVO_4:Nd was made at 1200 °C for 10 hours in ambient pressure to increase the optical transmittance of crystal. The grown YVO_4:Nd single crystal was split into a thickness of 2 mm in the a-axis and used in NMR experiments.

The static ^{51}V NMR spectra of YVO_4:Nd single crystals were observed by employing the Bruker 400 MHz Solid state Fourier transform (FT) NMR spectroscopy. The carrier frequency was set at $\omega_0/2\pi = 105.177$ MHz which is the Lamor frequency of the ^{51}V nucleus at

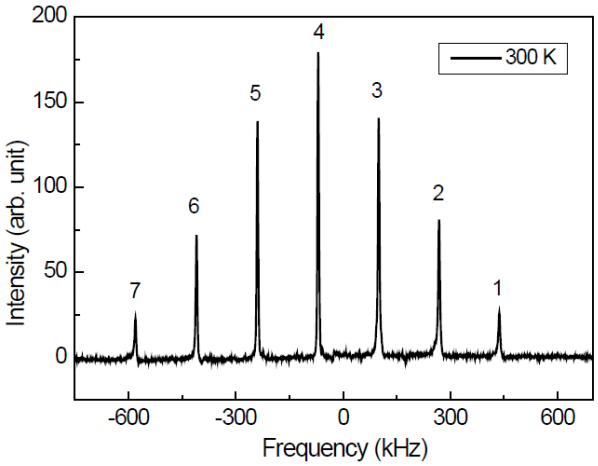

Fig. 2. Typical FT-NMR spectra of the ^{51}V in a YVO_4:Nd single crystal at 300 K. The zero point shows the Lamor frequency of the ^{51}V nucleus, $\omega_0/2\pi = 105.177$ MHz.

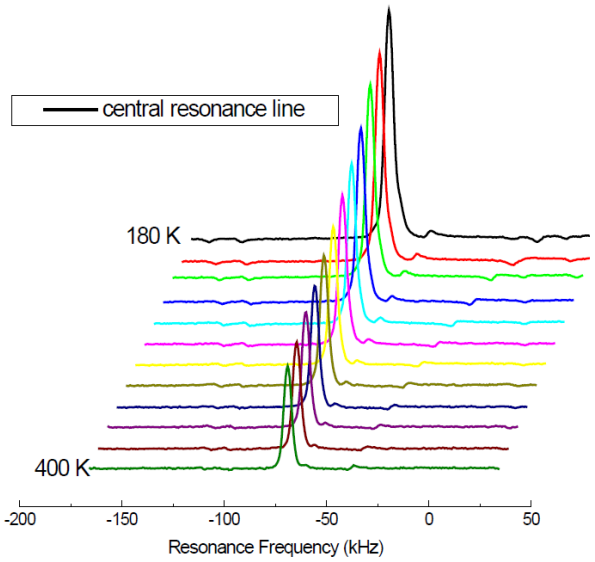

Fig. 3. (Color online) Intensity of the central resonance lines of the ^{51}V NMR spectra in a YVO_4:Nd single crystal as a function of temperature with 20 K interval.

the static magnetic field 9.4 T. The spin–lattice relaxation times T_1 of the ^{51}V in the laboratory frame were obtained using the saturation-recovery pulse sequence $(\pi/2 - t - \pi/2)$. The magnetization $M(t)$ of the ^{51}V nucleus at time t after the $\pi/2$ pulse was observed from the saturation recovery sequence. The $\pi/2$ pulse width was 1.6 μs for ^{51}V NMR. The temperature-dependent NMR measurements of the ^{51}V nucleus were examined in the range 180 $\sim$ 410 K. The nuclear magnetization recovery traces of ^{51}V in YVO_4:Nd were obtained as a function of delay time t at 300 K. The saturation recovery traces for only 5 nuclear magnetic resonance lines of ^{51}V nuclei from the nuclear quadrupole interaction are shown in Fig. 1 for different delay times from 1 s to 100 s. Magnetization of ^{51}V nuclei at time t = 100 s is almost fully saturated as shown in the inset of Fig. 1.

The NMR spectra of ^{51}V (I = 7/2, natural abundance 99.76%) in YVO_4:Nd single crystal were obtained in the experimental temperature range. One of the typical NMR spectrum of ^{51}V in YVO_4:Nd crystal at 300 K is shown in Fig. 2. This is a FT of the free induction decay (FID) for ^{51}V NMR. Only one set of NMR spectrum, which consists of 7 resonance lines, of ^{51}V in YVO_4:Nd crystal was obtained at all temperature ranges investigated. This means that there is no magnetically inequivalent V site in our YVO_4:Nd single crystal. The NMR spectrum has a central line and six equally spaced satellite lines. The levels denoted by 1, 2, 3, 4, 5, 6, and 7 correspond to the quantum states $M = |-7/2>$, $|-5/2>$, $|-3/2>$, $|-1/2>$, $|1/2>$, $|3/2>$, $|5/2>$, and $|7/2>$, respectively, for I = 7/2. The interval between the outer most satellite lines (frequency between $< -7/2|$ and $< 7/2|$) is 1017.183 kHz. The intensity ratio of the central and six satellite lines resonance line of the ^{51}V nucleus (I = 7/2) is theoretically 7 : 12 : 15: 16 : 15 : 12 : 7 with the first-order electric quadrupole interaction [20]. However, the intensity ratio of seven resonance lines for the ^{51}V NMR in Fig. 2 is 7 : 22 : 39 : 50 : 39 : 22 : 7 in our experiments because it is practically impossible to excite all of the 7 resonance lines equally.

The intensity of the central resonance line decreases as the temperature increases as shown in Fig. 3. Only the central resonance line of ^{51}V NMR spectra is shown in Fig. 3 with 20 K interval from 180 K to 400 K. The zero point of the frequency in Figs. 2 and 3 shows the resonance frequency, 105.177 MHz, of the bare ^{51}V nucleus. The resonance frequency of a nucleus is different from that of a nucleus embedded in crystal from that for a 'bare' nucleus. These frequency shifts from the zero point in Fig. 3 originate from the chemical shift [21]. The linewidth (full width at half maximum, FWHM) of the central line for ^{51}V resonance line at 300 K is $\Delta\nu_{FWHM}$ = 4.724 kHz, recorded with a pulse frequency of 105.177 MHz as shown in Fig. 4. The linewidth of

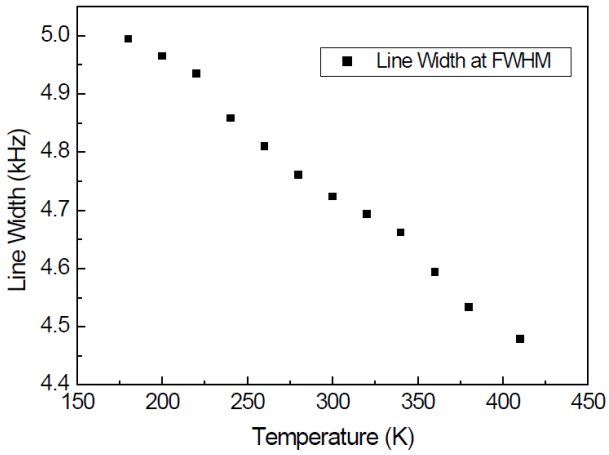

Fig. 4. Linewidth $\Delta\nu_{FWHM}$ of the ^{51}V NMR spectrum in a YVO_4:Nd single crystal as a function of temperature.

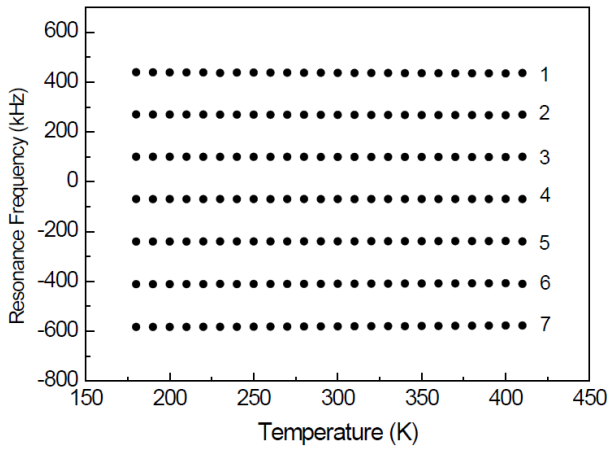

Fig. 5. Temperature dependence of the Zeeman splitting for the ^{51}V NMR spectrum in a YVO_4:Nd single crystal. The zero point of vertical axis represents the Lamor frequency of the ^{51}V nucleus, $\omega_0/2\pi = 105.177$ MHz.

the central resonance line for ^{51}V in YVO_4:Nd crystal decreases as temperature increases from 180 K to 410 K. It is common to see motional narrowing of the ^{51}V nuclei NMR linewidth with increasing temperature. Motional narrowing is a phenomenon where a certain resonance frequency has a smaller linewidth than expected, due to motion in an inhomogeneous system [22]. When the ^{51}V atoms are diffusing throughout the spin-system, the linewidth is narrower than what it would have been if the atoms were stationary. Motional narrowing effect is more active when the temperature increases.

The line splitting between the satellite and central resonance lines of the ^{51}V resonance lines showing the ^{51}V nuclear quadrupole interaction was found to decrease slightly as temperature increases over all temperature range as shown in Fig. 5. This means that the quadrupole interaction (splitting) of ^{51}V nucleus decreases slightly and the local structure around the ^{51}V atom changes slightly with increasing temperature. The splitting between 1 and 7 for 180 K and 410 K are 1022.15 kHz and 1013,44 kHz, respectively. The central resonance line, the transition between $-|1/2>$ and $|1/2>$, was not affected by nuclear quadrupole interaction, unlike the satellite resonance lines which were shifted. The decreasing quadrupole coupling constant with increasing temperature observed in our empirical results (see Fig. 5) can be predicted by the Bayer theory [23–25] because the vibration amplitude of a rigid body increases as temperature increases.

III. ANALYSIS AND DISCUSSION

The spin-lattice relaxation time of ^{51}V in YVO_4:Nd was examined by the saturation recovery method as a function of temperature. The magnetization recovery curve of the ^{51}V nuclei displays the paramagnetic impurity relaxation behavior in the short delay time range. Fig. 6 shows the relaxation processes at 180 K and 300 K. The rapidly decreasing range during the relaxation process in Fig. 6(a) and the linearly increasing range in Fig. 6(b) represent the paramagnetic relaxation effect suggested by Blumberg in diffusion-limited relaxation [26]. The magnetization $M(t)$ at 180 K is shifted upwards so that it can be distinguished from the $M(t)$ at 300 K in Fig. 6(b). The T_1 value can be obtained with the following equation because the magnetization recoveries for ^{51}V nucleus fit a single exponential function:

$$[M(0)–M(t)]/2M(0) = \exp(-t/T_1) \qquad (1)$$

where $M(0)$ is the saturated nuclear magnetization when the full recovery is achieved and $M(t)$ is the magnetization. The spin-lattice relaxation time (T_1) values are obtained with Eq. (1) and shown in Fig. 7. The relaxation time of ^{51}V increases slightly until the temperature reaches 280 K, and subsequently decreases until 410 K. At temperatures higher than 280 K, $1/T_1$ is directly proportional to the squared value of temperature as shown

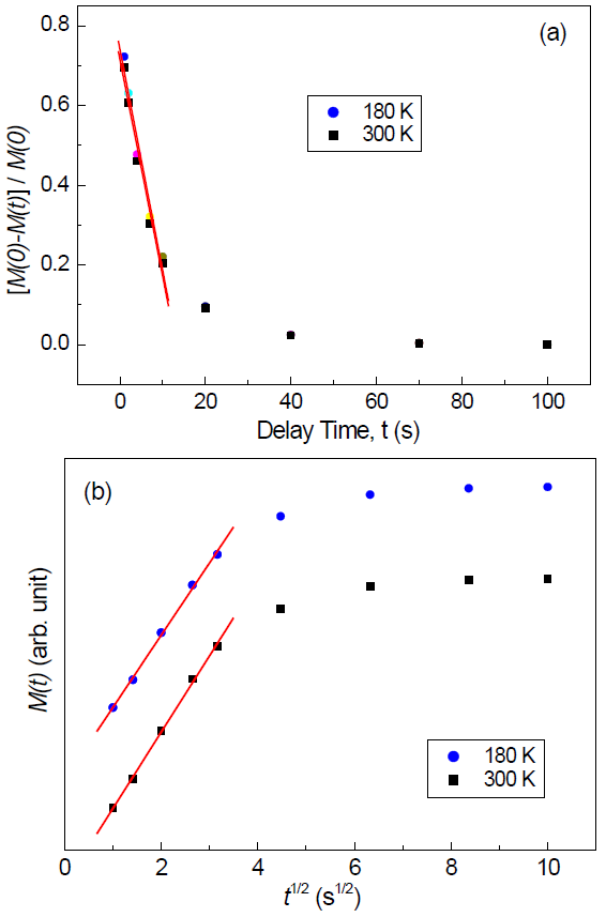

Fig. 6. (Color online) (a) The normalized magnetization and (b) magnetization recovery graphs at 180 K and 300 K for the ^{51}V nucleus in a YVO_4:Nd single crystal. $M(0)$ is the saturated magnetization.

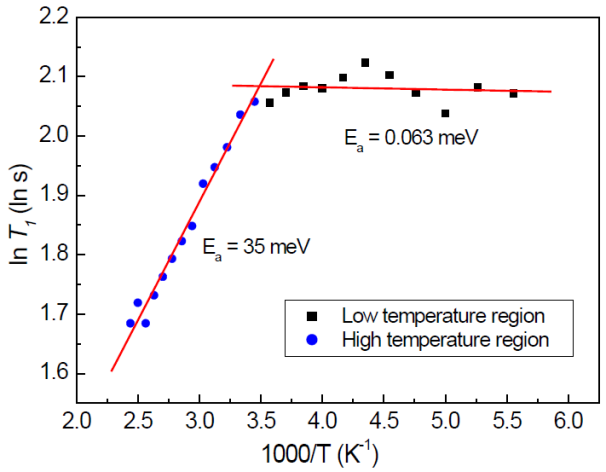

Fig. 7. (Color online) The spin-lattice relaxation time of the ^{51}V nucleus in a YVO_4:Nd single crystal as a function of inverse temperature. Activation energy of the ^{51}V nucleus is also obtained at two different temperature regions.

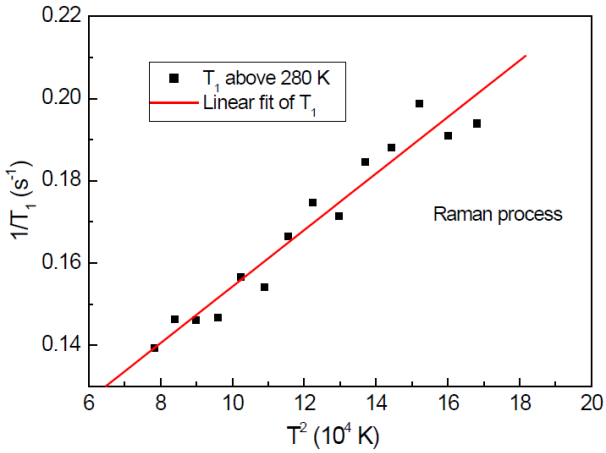

Fig. 8. (Color online) The spin lattice relaxation rate of the ^{51}V in a YVO_4:Nd single crystal as a function of temperature squared.

in Fig. 8. The Raman process, or the relaxation occurring from the two-phonon process, gives the relaxation rate which is proportional to temperature squared in the high temperature limit [27–30].

Since $\ln T_1$ of ^{51}V nucleus is almost proportional to the inverse temperature, under the assumption that T_1 and the correlation time t have a linear relationship, we can deduce E_a of ^{51}V by the Arrhenius equation:

$$\tau = \tau_0 \exp \frac{E_a}{\kappa T} \qquad (2)$$

The activation energies E_a obtained from 180 K to 280 K is 0.063 meV, whereas E_a above 280 K is 35 meV. The smaller activation energy from 180 K up to 280 K suggests that there exists some other relaxation mechanism preferred at lower temperatures.

The Nd^{3+} paramagnetic impurity contribution to the relaxation mechanism of ^{51}V nucleus up to 280 K dominates the nuclear quadrupole relaxation, which is induced by thermally activated phonons. The quantity C, which is the interaction strength between an impurity ion and a nucleus, is defined by the following equation [31]:

$$\tau^{-1}(r) = Cr^{-6} \qquad (3)$$

where $\tau^{-1}(r)$ denotes the relaxation rate of a single nucleus and r denotes the distance between the impurity ion and the nucleus. In a powder sample, C is given by [32]

$$C = \frac{2}{5}\gamma_p^2\gamma_n^2\hbar^2 J(J+1)\left[\frac{\tau_i}{1+\omega_0^2\tau_i^2} + \frac{7\tau_i}{3(1+\omega_e^2\tau_i^2)}\right] \qquad (4)$$

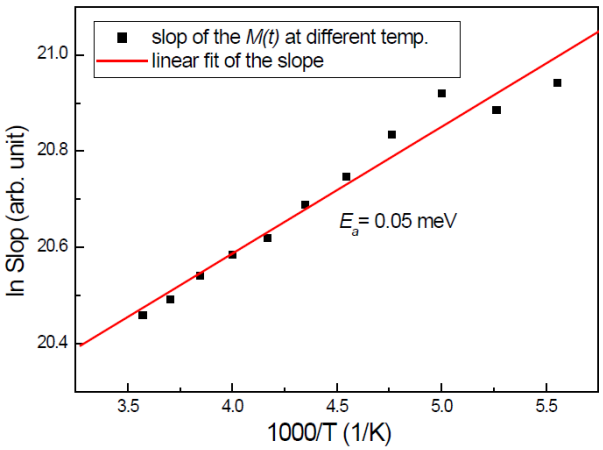

Fig. 9. (Color online) The Semi-log plot of the slope (see the straight lines at 180 K and 300 K in Fig. 6) for the ^{51}V nucleus *vs.* the inverse temperature at low temperatures below 280 K.

Here, the γ_n denotes the gyromagnetic ratio, J the angular momentum, γ_p the gyromagnetic ratio, γ_i the spin-lattice relaxation time, and ω_e the Larmor frequency of the paramagnetic ion. After the disturbance of the nuclear magnetization, any given nucleus will be first affected by the nearest paramagnetic impurity ions for a short time [26]. Three cases are possible for the nuclear relaxation caused by paramagnetic impurity ions. Firstly, if the delay time t is not long enough for the occurrence of the spin diffusion as in our case, the relaxation process acts as if there is no spin diffusion at all. This indicates that the magnetization follows the equation below for small t values [26]:

$$M_z(t) \simeq \left(\frac{4\pi^{3/2}}{3}\right) NC^{1/2}t^{1/2} \qquad (5)$$

where N denotes the paramagnetic ion concentration. The slope of each temperature in the recovery curve can be calculated as depicted in Fig. 6(b). The gradients can be obtained from the straight line plotted in the short time region. In Eq. (4), C has a close relationship to the spin–lattice relaxation time of the paramagnetic impurity ion. Generally, ω_e is several hundred times larger than ω_0. We assumed that C is directly proportional to $1/\tau_i$ from the first term in the brackets of Eq. (4). Therefore, by examining Eqs. (2) - (5), we could deduce that the gradient of the straight line in Fig. 6(b) is directly proportional to C^2 and to $\exp(-E_a/2kT)$. In Fig. 9, the x-axis is $1/T$ in Kelvin and the y-axis is the gradient in natural logarithm. From the slopes in the graph above, we calculated the activation energy to be E_a = 0.05 meV, which is the minimum energy required to activate the paramagnetic ion Nd^{3+} and enable it to take part in the spin lattice relaxation of ^{51}V. This result is considerably close to the E_a (0.063 meV) obtained from Fig. 7. This means that the two values 0.05 meV and 0.063 meV show correspondence, hinting that they have the same relaxation mechanism. Therefore, the Nd^{3+} paramagnetic relaxation is the predominant below 280 K. That is, the E_a of the paramagnetic ions was obtained from the magnetization recovery curve of ^{51}V in the YVO_4:Nd crystal.

IV. SUMMARY

The nuclear magnetic resonance of ^{51}V nuclei in a YVO_4:Nd crystal has been explored in the range 180 K ∼ 410 K by a FT NMR spectrometer. Only one set of ^{51}V NMR spectrum (seven resonance lines from quadrupole splitting) was recorded. This means that there is only one magnetically equivalent ^{51}V center in the YVO_4:Nd crystal. The linewidth (FWHM) as well as peak-to-peak intensity of ^{51}V NMR spectrum decrease as temperature increases. The nuclear quadrupole splitting of ^{51}V nucleus is slightly decreased when temperature increases in the temperature range. This reveals that the quadrupole interaction of the ^{51}V nucleus in the YVO_4:Nd crystal decreases with increasing temperature.

In the ^{51}V nuclear magnetic resonance relaxation study on YVO_4:Nd, the spin lattice relaxation mechanisms of ^{51}V were examined. Furthermore, the influence of the Nd^{3+} paramagnetic impurity ion on the ^{51}V nuclear relaxation is studied using an NMR method. While the quadrupolar interaction through the Raman process on the ^{51}V nuclear relaxation is predominant beyond 280 K, the paramagnetic impurity effect on the ^{51}V nuclear relaxation is predominant under 280 K. This was verified through the examination of the activation energy of the paramagnetic impurity ions as well as that of the ^{51}V nucleus in the YVO_4:Nd single crystal at low temperatures (below 280 K). The calculated activation energy for the ^{51}V nucleus below and above 280 K are 0.0628 meV and 34.9 meV, respectively.

REFERENCES

[1] Z. Wang, L. Sun, S. Zhang, X. Meng and R. Cheng *et al.*, Opt. Laser Technol. **33**, 47 (2001).

[2] H. Zhang, J. Wang, C. Wang, L. Zhu and X. Hu *et al.*, Opt. Mater. **23**, 449 (2003).

[3] J. D. Kinsley and G. W. Ludwig, J. Appl. Phys. **41**, 370 (1970).

[4] P. P. Yaney and L. G. DeShazer, J. Opt. Soc. Am. **66**, 1405 (1976).

[5] H. Nagamoto, M. Nakatsuka, K. Naito, M. Yamanaka and K. Yoshida *et al.*, Rev. Laser Eng. **18**, 639 (1990).

[6] A. W. Tucker, M. Brinbaum, C. L. Fincher and J. W. Erler, J. Appl. Phys. **48**, 4907 (1977).

[7] R. A. Fields, M. Bimbaum and C. L. Fincher, Appl. Phys. Lett. **51**, 1885 (1987).

[8] J. R. Oconnor, Appl. Phys. Lett. **9**, 407 (1966).

[9] T. Kojima, T. Sasaki, S. Nakai and Y. Kuwano, Appl. Phys. **59**, 1235 (1990).

[10] T. Sasaki, T. Kojima, A. Yokotani, O. Ogur and S. Nakai, Opt. Lett. **16**, 1665 (1991).

[11] V. I. Popov, K. S. Bagdasarov, I. N. Guseva and M. V. Mokhosoev, Krisallografia **13**, 1109 (1968)

[12] B. M. Wanklyn, J. Cryst. Growth **54**, 610 (1981).

[13] J. Lories and M. Vichr, J. Cryst. Growth **13-14**, 593 (1972).

[14] K. Robinson, G. V. Gibbs and P. H. Ribbe, Am. Mineral **56**, 782 (1971).

[15] T. Shonai, M. Higuchi and K. Kodaira, J. Cryst. Growth **233**, 477 (2001).

[16] B. Q. Hu, Y. Z. Zhang, X. Wu and X. L. Chen, J. Cryst. Growth **226**, 511 (2001).

[17] B. C. Chakoumakos, A. M. Marvin, L. A. Boatner, J. Solid State Chem. **109**, 197 (1994).

[18] W. Ryba-Romanowski, R. Lisiecki, H. Jelinkova and J. Sulc, Prog. Quantum Electron. **35**, 109 (2011).

[19] S. Zhang, J. Gu, G. Jia and Z. Liu, Opt. Mater. **39**, 178 (2015).

[20] S. H. Choh, *Solid State Magnetic Resonance* (Korea University Press, Seoul, 2003), Chap. 2.

[21] A. Abragam, *The Principles of Nuclear Mngnetism* (Oxford University Press, Oxford, 1961), Chaps. VI, VI1, IX.

[22] E. Yablonovitch, Nature **550**, 458 (2017).

[23] H. Bayer, Z. Physik **130**, 227 (1951).

[24] T. C. Wang, Phys. Rev. **99**, 566 (1955).

[25] T. P. Das and E. L. Han, *Nuclear Quadrupole Resonance Spectroscopy* (Academic Press, New York, 1958), Chap. 1.

[26] W. E. Blumberg, Phys. Rev. **119**, 79 (1960).

[27] J. Van Kranendonk, Physica **20**, 781 (1954).

[28] A. Abragam, *The Principles of Nuclear Magnetism* (Oxford University Press, Oxford, 1961), Chaps I, IX.

[29] R. L. Mieher, Phys. Rev. **125**, 1537 (1962).

[30] T. H. Yeom, K. S. Hong, I. Yu, H. W. Shin and S. H. Choh, J. Appl. Phys. **82**, 2472 (1997).

[31] T. T. Phua, B. J. Beaudry, D. T. Peterson, D. R. Torgeson and R. G. Barnes *et al.*, Phys. Rev. B **28**, 6227 (1983).

[32] N. Bloembergen, Physica **15**, 386 (1949).